Polygenic Effects of the Lipid Metabolic Pathway Accelerated Pathological Changes and Disrupted Default Mode Network Trajectory Across the Alzheimer's Disease Spectrum

Feifei Zang, PhD[a]; Yao Zhu, PhD[a]; Xinyi Liu, PhD[a]; Dandan Fan, PhD[a]; Qing Wang, PhD[a]; Qianqian Zhang, MD[a]; Cancan He, PhD[a]; Zhijun Zhang, MD, PhD[a,b]; and Chunming Xie, MD, PhD,[a,b,*] on behalf of Alzheimer's Disease Neuroimaging Initiative[c] and the Alzheimer Disease Metabolomics Consortium[c]

ABSTRACT

Objective: Dyslipidemia is a controversial risk for Alzheimer's disease (AD) with unknown mechanisms. This study aimed to investigate polygenic effects of the lipid metabolic pathway on cerebrospinal fluid (CSF) core biomarkers, cognition, and default mode network (DMN).

Methods: Cross-sectional data on serum lipids, CSF core biomarkers, and functional MRI findings for 113 participants (25 cognitively normal, 20 with subjective cognitive decline, 24 early amnestic, 23 with late mild cognitive impairment, and 21 with AD) from the Alzheimer's Disease Neuroimaging Initiative were included. Different cognitive stages were categorized based on neuropsychological assessments. Multivariable linear regression analyses were conducted to investigate the polygenic and interactive effects on the DMN. The correlations of lipid-related polygenes and serum lipids with cognitive performance were also studied via regression analyses.

Results: The polygenic scores were significantly correlated with CSF levels of core biomarkers ($P < .05$) but not with cognition. Several serum lipids were associated with total tau. CSF core biomarkers and 6 serum lipids both could impact cognition in a nonlinear manner. Polygenic effects exhibited diverse trajectories on the DMN subsystems across the AD spectrum. Extensive genetic and interactive effects were mainly concentrated in the cortical frontal-parietal network and subcortical regions. Brain regions of lipid metabolites linking to DMN involved sensorimotor network and occipital lobe.

Conclusions: Polygenic effects of the lipid metabolic pathway could accelerate pathological changes and disrupted DMN subsystem trajectory across the AD spectrum. These results deepen the understanding of the mechanism of lipid metabolism affecting the neural system and provide several lipid indicators that enable the impairments of lipid metabolism on the brain to be monitored.

J Clin Psychiatry 2021;82(6):20m13739

To cite: Zang FF, Zhu Y, Liu XY, et al. Polygenic effects of the lipid metabolic pathway accelerated pathological changes and disrupted default mode network trajectory across the Alzheimer's disease spectrum. *J Clin Psychiatry*. 2021;82(6):20m13739.

To share: https://doi.org/10.4088/JCP.20m13739

[a]Department of Neurology, Affiliated ZhongDa Hospital, School of Medicine, Southeast University, Nanjing, Jiangsu, China

[b]Neuropsychiatric Institute, Affiliated ZhongDa Hospital, Southeast University, Nanjing, Jiangsu, China

[c]See end of article for a list of the group members.

**Corresponding author:* Chunming Xie, MD, PhD, No.87 Dingjiaqiao Rd, Nanjing, China, 210009 (chmxie@163.com).

Accumulating evidence from previous studies has indicated that an increased plasma lipid level is a high-risk factor for Alzheimer's disease (AD).[1–5] The progressive deterioration of lipid homeostasis may be a potential therapeutic target for AD prevention.[6] Due to the presence of the blood-brain barrier, transport of lipid-related metabolites between the cerebral circulation and cerebrospinal fluid (CSF) hardly exists. Yet, many studies have shown that lipids affect β-amyloid (Aβ) and tau pathology.[7–11] Hence, disturbance of lipid metabolism may accelerate pathological damage to the brain. The lipid metabolism disorder hypothesis is complementary to those mainstream hypotheses in AD. The level of blood lipids may partly reflect the state of lipid metabolism in the body. Because lipids are easy to detect in clinical practice, they are becoming biomarkers for monitoring disease progression.[12] Early intervention on the risk factors of hyperlipidemia may be helpful to delay the onset of AD in the preclinical stage and provide an early time window for the prevention and treatment of AD.

A single gene strategy is unable to explain the complex mechanism of AD for its genetic heterogeneity. The pathway-based polygenic combination approach might address this issue. Genetic risk score (GRS) has been used to combine effects of multiple minor variants to explore the relationship of pathway-specific GRS and biological markers with cognitive function.[13] This study also investigates the genetic protective score (GPS) and the relative risk score (RRS, equals GRS minus GPS) to explore the mechanism underlying the gene-disease interaction from a novel perspective.

Lipid-related brain imaging studies[14,15] have also provided more opportunities to understand the pathogenesis of AD. Structural magnetic resonance imaging (MRI) evidence demonstrated that higher levels of triglycerides in midlife were associated with smaller brain volumes.[16] A diffusion tensor imaging study[17] found that higher levels of low-density lipoprotein cholesterol and triglycerides and lower levels of high-density lipoprotein cholesterol were related to lower axial diffusivity in multiple white matter regions. The default mode network (DMN), as an intrinsic brain network, is not homogeneous but is composed of several dissociated subnetworks with separate functions.[18,19] The posterior DMN (pDMN) but not the anterior DMN (aDMN) might initiate network cascading deterioration throughout the disease spectrum,[20] and how connectivity is affected in these subsystems might depend on the stage of AD.[21] However, owing to the asynchrony within DMN subsystems, the impact of GRS on the subnetworks might be distinct, which has not been reported.

Clinical Points

- Abnormalities of lipid metabolism in Alzheimer's disease are common.
- Lipid-related genes and serum lipids may affect cognitive function via regulating brain networks.
- Targeting lipid metabolism with pharmacologic and nonpharmacologic interventions may provide an effective strategy for the treatment of Alzheimer's disease spectrum patients.

To better understand the pathophysiology of the AD spectrum, we incorporated various levels ranging from genetic (GRS, GPS, and RRS), molecular (CSF and serum lipids biomarkers), neuroimaging (aDMN and pDMN), and cognitive aspects. We hypothesized that the lipid metabolism–related polygenes may be a candidate cause for disrupted brain networks and impaired cognitive performance. Here, we aimed first to explore the relationships between lipid metabolic pathway–based polygenic effects with molecular biomarkers and cognition, and second to investigate the effect of GPS, GRS, and RRS of lipid metabolic pathways on the DMN subnetworks across the AD spectrum.

METHOD

Participants

Cross-sectional data at baseline were obtained from the Alzheimer's Disease Neuroimaging Initiative (ADNI) database (http://adni.loni.usc.edu) before November 15, 2019. A total of 113 subjects were included for the final analysis, including 25 cognitively normal (CN), 20 with subjective cognitive decline (SCD), 24 with early amnestic mild cognitive impairment (EMCI), 23 late mild cognitive impairment (LMCI), and 21 with AD. Different cognitive stages were categorized based on neuropsychological assessments. Detailed information was available in the ADNI-2 protocol (http://adni.loni.usc.edu/wp-content/themes/freshnews-dev-v2/documents/clinical/ADNI-2_Protocol.pdf). Participant flow is illustrated in Supplementary Figure 1. Institutional review boards approved study procedures, and written informed consent was obtained for all participants.

Demographic, Behavioral, Genetic, and Molecular Data

Demographic information (age, sex, and education) was obtained and general cognitive assessments (Mini-Mental State Examination [MMSE] and Alzheimer's Disease Assessment Scale–13-item cognitive subscale[ADAS-cog]) were completed at baseline.[22] Based on the lipid metabolism hypothesis, 10 single nucleotide polymorphisms (SNPs) from 9 candidate genes were retrieved: *CLU*,[23] *LDLR*,[24] *LRP1*,[25] *PICALM*,[23] *APOE*,[26] *SORL1*,[27] *CETP*,[28] *ABCA1*,[29] and *BIN1*.[30] SNP genotyping for all genes was performed according to the manufacturer protocols.[31] SNPs were excluded if the minor allele frequency (MAF) was less than 5%. Hardy-Weinberg equilibrium (HWE) for each respective gene was calculated with χ^2. Summary information regarding lipid-related genes is shown in Supplementary Table 1. The CSF core biomarkers with Aβ, total tau (t-tau), and tau phosphorylated at the threonine-181 position (p-tau) and serum lipids markers were also recruited. An odds ratio (OR) greater than 1 indicates a higher risk of this locus for disease. An OR less than 1 indicates that the allele mutation is a relative protective factor, and people with this allele change have a lower risk of developing disease. Using the effect size OR as weight, a weighted polygenic score was constructed as the sum of the products of SNP dosages from genotype and their corresponding weights.[32] After exclusion of incomplete or missing information regarding serum lipids and ratio values, 35 lipid markers were sorted out for final analysis.

Resting-State Functional MRI

All resting-state functional MRI (rs-fMRI) images were recruited from the ADNI-GO and ADNI-2 projects. The gradient-echo planar imaging sequence parameters were as below: flip angle = 80°, matrix = 64 × 64, pixel space = 3.3 × 3.3 × 3.3 mm^3, number of slices = 48, slice thickness = 3.3 mm, repetition time (TR) = 3,000 ms, echo time (TE) = 30 ms, and time points = 140.

The rs-fMRI data pre-process was under SPM12 (https://www.fil.ion.ucl.ac.uk/spm/software/spm12/) and RESTplusV1.24[33] (http://www.restfmri.net/forum/restplus) in MATLAB 2012b (MathWorks, Inc; Natick, Massachusetts). After the general preprocessing pipeline, including removing the first 10 time points, head motion correction, spatial normalization, and smoothness, the smoothed data were further decomposed into functional networks using group-level spatial independent component analysis (ICA) as implemented in the GIFTv4.0b software (http://mialab.mrn.org/software/gift/). The WFU PickAtlas Tool v2.4 (NITRC) was used to construct aDMN and pDMN templates. We used sorting criteria of multiple linear regression[34] to select the optimal spatial independent component that matches aDMN and pDMN templates best. Then, all subject-specific spatial maps and time courses were sorted out.

Statistical Analysis

Demographic and neuropsychological data analysis. One-way analysis of variance (ANOVA) was used to compare separately group differences in age, education, MMSE and ADAS-cog scores, Aβ levels, CSF total tau and p-tau levels, and blood lipid metabolites. Chi-square tests were used to separately compare group differences in sex and the 9 candidate genotypes. Significance levels were set at $P < .05$. Post hoc analyses with the least significant difference correction ($P < .05$) were deemed significant between pairs of groups. Statistical analyses were conducted using SPSS 25 software (SPSS, Inc; Chicago, Illinois).

Phenotypic regression analyses. To investigate the correlations between pairs of polygenic scores (PGSs), serum lipid metabolites, CSF core biomarkers, and cognitive

Table 1. Demographic, Behavioral, Genetic, and Molecular Biomarkers*

Item	CN (n = 25)	SCD (n = 20)	EMCI (n = 24)	LMCI (n = 23)	AD (n = 21)	*P* Value
Age, y	74.64 ± 6.10	72.75 ± 5.73	69.96 ± 7.15	70.78 ± 6.99	71.81 ± 7.77	.147
Sex, male/female	12/13	9/11	11/13	14/9	12/9	.764**
Education, y	16.56 ± 2.22	16.65 ± 3.05	15.46 ± 2.50	16.52 ± 2.57	15.14 ± 2.76	.172
MMSE score	28.56 ± 1.33[a]	29.15 ± 0.93[b,c,d]	27.88 ± 2.12[e]	27.83 ± 1.59[f]	22.67 ± 2.50	< .001
ADAS-cog score	9.44 ± 3.43[a,g,h]	8.65 ± 3.50[b,c,d]	13.17 ± 5.68[e,i]	16.87 ± 5.29[f]	35.81 ± 8.99	< .001
Multiple protective genes, yes/no, n						
CLU rs11136000 T (TC + TT/CC)	17/8	16/4	16/8	15/8	13/8	.775**
LDLR rs5930 A (AG + AA/GG)	19/6	14/6	15/9	13/10	11/10	.452**
LRP1 rs1799986 T (TC + TT/CC)	8/17	5/15	8/16	3/20	10/11	.152**
PICALM rs3851179 A (AG + AA/GG)	14/11	11/9	15/9	13/10	11/10	.972**
Multiple risk genes, yes/no, n						
APOE ε4 (±)	7/18	5/15	14/10	10/13	15/6	.008**
SORL1 rs2070045 G (TG + GG/TT)	9/16	8/12	11/13	10/13	6/15	.785**
CETP rs5882 A (AG + AA/GG)	21/4	19/1	23/1	20/3	19/2	.631**
ABCA1 rs2230808 G (AG + GG/AA)	21/4	19/1	23/1	19/4	19/2	.491**
BIN1 rs744373 C (TC + CC/TT)	10/15	13/7	15/9	14/9	11/10	.407**
Cerebrospinal fluid metabolites, pg/mL						
Aβ	180.46 ± 48.60[a,j]	211.25 ± 50.10[b,c,d]	177.50 ± 47.77[e]	167.60 ± 53.17	140.40 ± 43.59	< .001
Total tau	72.92 ± 38.50[a]	67.33 ± 23.02[d]	81.00 ± 53.68[e]	85.17 ± 50.23[f]	129.29 ± 61.42	< .001
p-tau	36.91 ± 19.13[a]	31.32 ± 9.31[d]	41.10 ± 25.19[e]	44.48 ± 24.38	55.23 ± 26.13	.01
Serum lipid metabolites, mmol/L						
Medium VLDL particles	0.93 ± 0.39	0.93 ± 0.47	1.03 ± 0.47	1.04 ± 0.48	0.97 ± 0.40	.860
Small VLDL particles	1.05 ± 0.30	1.11 ± 0.37	1.18 ± 0.41	1.14 ± 0.35	1.12 ± 0.34	.783
Very small VLDL particles	0.96 ± 0.20	1.10 ± 0.22	1.02 ± 0.26	0.98 ± 0.21	1.01 ± 0.24	.346
IDL particles	2.13 ± 0.53	2.47 ± 0.51	2.25 ± 0.64	2.16 ± 0.53	2.24 ± 0.62	.350
Large LDL particles	2.53 ± 0.65	2.91 ± 0.63	2.70 ± 0.80	2.57 ± 0.65	2.66 ± 0.70	.417
Medium LDL particles	1.46 ± 0.39	1.66 ± 0.38	1.58 ± 0.49	1.49 ± 0.40	1.53 ± 0.39	.493
Small LDL particles	0.95 ± 0.24	1.07 ± 0.24	1.03 ± 0.30	0.96 ± 0.24	0.99 ± 0.24	.491
Large HDL particles	2.07 ± 0.68	2.03 ± 0.69	1.83 ± 0.79	1.85 ± 0.99	1.89 ± 0.72	.759
Medium HDL particles	2.27 ± 0.35	2.22 ± 0.33	2.26 ± 0.50	2.22 ± 0.47	2.15 ± 0.28	.886
Small HDL particles	2.62 ± 0.24	2.60 ± 0.20	2.72 ± 0.22	2.66 ± 0.20	2.61 ± 0.21	.352
Serum total cholesterol	3.65 ± 0.73	4.01 ± 0.68	3.79 ± 0.80	3.64 ± 0.72	3.72 ± 0.83	.497
Total cholesterol in VLDL	0.46 ± 0.14	0.53 ± 0.18	0.52 ± 0.20	0.51 ± 0.17	0.50 ± 0.17	.734
Remnant cholesterol (non-HDL, non-LDL cholesterol)	0.95 ± 0.25	1.11 ± 0.27	1.04 ± 0.34	1.01 ± 0.28	1.02 ± 0.30	.511
Total cholesterol in LDL	1.19 ± 0.35	1.38 ± 0.34	1.29 ± 0.43	1.21 ± 0.35	1.26 ± 0.36	.436
Total cholesterol in HDL	1.50 ± 0.25	1.52 ± 0.29	1.45 ± 0.35	1.43 ± 0.38	1.44 ± 0.28	.847
Total cholesterol in HDL_2	1.03 ± 0.23	1.04 ± 0.27	0.98 ± 0.33	0.96 ± 0.35	0.97 ± 0.25	.839
Total cholesterol in HDL_3	0.47 ± 0.02	0.48 ± 0.02	0.47 ± 0.03	0.47 ± 0.03	0.47 ± 0.02	.738
Esterified cholesterol	2.55 ± 0.53	2.82 ± 0.50	2.66 ± 0.58	2.55 ± 0.52	2.60 ± 0.59	.474
Free cholesterol	1.10 ± 0.20	1.19 ± 0.19	1.13 ± 0.22	1.09 ± 0.20	1.12 ± 0.24	.559
Serum total triglycerides	1.03 ± 0.35	1.01 ± 0.37	1.08 ± 0.37	1.10 ± 0.37	1.05 ± 0.33	.916
Triglycerides in VLDL	0.66 ± 0.28	0.63 ± 0.31	0.71 ± 0.30	0.73 ± 0.32	0.67 ± 0.27	.822
Triglycerides in LDL	0.15 ± 0.04	0.16 ± 0.03	0.15 ± 0.03	0.15 ± 0.03	0.15 ± 0.04	.948
Triglycerides in HDL	0.12 ± 0.03	0.12 ± 0.02	0.12 ± 0.03	0.12 ± 0.03	0.12 ± 0.03	.964
Total phosphoglycerides	1.72 ± 0.30	1.80 ± 0.27	1.73 ± 0.29	1.68 ± 0.31	1.70 ± 0.30	.748
Phosphatidylcholine and other cholines	1.65 ± 0.28	1.75 ± 0.26	1.66 ± 0.27	1.62 ± 0.29	1.64 ± 0.29	.635
Sphingomyelins	0.37 ± 0.05	0.39 ± 0.06	0.37 ± 0.07	0.36 ± 0.07	0.36 ± 0.07	.627
Total cholines	2.06 ± 0.30	2.16 ± 0.28	2.05 ± 0.30	2.00 ± 0.31	2.04 ± 0.33	.563
Total fatty acids	9.73 ± 1.85	10.30 ± 1.78	10.13 ± 1.83	9.87 ± 1.90	9.90 ± 1.92	.856
Docosahexaenoic acid	0.12 ± 0.04	0.13 ± 0.04	0.12 ± 0.03	0.12 ± 0.04	0.12 ± 0.04	.996
Linoleic acid	2.68 ± 0.46	2.85 ± 0.45	2.85 ± 0.48	2.73 ± 0.44	2.74 ± 0.59	.692
Omega-3 fatty acids	0.39 ± 0.14	0.40 ± 0.12	0.41 ± 0.10	0.40 ± 0.13	0.40 ± 0.13	.995
Omega-6 fatty acids	3.26 ± 0.53	3.48 ± 0.51	3.44 ± 0.54	0.30 ± 0.52	3.34 ± 0.64	.653
Polyunsaturated fatty acids	3.66 ± 0.64	3.88 ± 0.61	3.84 ± 0.62	3.70 ± 0.64	3.74 ± 0.75	.743
Monounsaturated fatty acids	2.56 ± 0.58	2.66 ± 0.58	2.69 ± 0.61	2.63 ± 0.62	2.60 ± 0.57	.946
Saturated fatty acids	3.51 ± 0.69	3.75 ± 0.64	3.59 ± 0.67	3.54 ± 0.69	3.56 ± 0.66	.796

*Unless indicated, data are presented as mean ± SD. Post hoc analyses were used with least significant difference (LSD) correction ($P < .05$). *P* values obtained using the χ^2 test are indicated by a double asterisk (**); other *P* values were obtained by 1-way ANOVA, but if the variance homogeneity test $P < .05$, the *P* value was acquired by Kruskal-Wallis test.

[a]Statistically significant difference was detected between CN group and AD group. [b]Statistically significant difference was detected between SCD group and EMCI group. [c]Statistically significant difference was detected between SCD group and LMCI group. [d]Statistically significant difference was detected between SCD group and AD group. [e]Statistically significant difference was detected between EMCI group and AD group. [f]Statistically significant difference was detected between LMCI group and AD group. [g]Statistically significant difference was detected between CN group and EMCI group. [h]Statistically significant difference was detected between CN group and LMCI group. [i]Statistically significant difference was detected between EMCI group and LMCI group. [j]Statistically significant difference was detected between CN group and SCD group.

Abbreviations: Aβ = amyloid β peptides 1 to 42, *ABCA1* = ATP-binding cassette transporter A1, AD = Alzheimer's disease, ADAS-cog = Alzheimer's Disease Assessment Scale–13-item cognitive subscale, ANOVA = analysis of variance, *APOE* = apolipoprotein E, *BIN1* = bridging integrator 1, *CETP* = cholesterol ester transfer protein, *CLU* = clusterin, CN = cognitively normal, EMCI = early mild cognitive impairment, HDL = high-density lipoprotein (HDL_2 and HDL_3 indicate HDL subfractions), IDL = intermediate-density lipoprotein, LDL = low-density lipoprotein, *LDLR* = low density lipoprotein receptor, LMCI = late mild cognitive impairment, *LRP1* = low density lipoprotein receptor-related protein 1, MMSE = Mini-Mental State Examination, *PICALM* = phosphatidylinositol-binding clathrin assembly protein, p-tau = tau phosphorylated at the threonine 181 position, SCD = subjective cognitive decline, *SORL1* = sortilin-related receptor 1, VLDL = very low density lipoprotein.

Figure 1. Regression Analyses Among Polygenic Scores, Serum Lipid Metabolites,[a] Cerebrospinal Fluid Core Biomarkers, and Cognitive Performance in the AD Spectrum*

A: Linear regression between polygenic scores and cerebrospinal fluid biomarkers revealed that the GPS was correlated with Aβ levels but not total tau and p-tau levels; in contrast, GRS was significantly correlated with total tau levels and marginally associated with Aβ levels but not with p-tau levels, while RRS significantly influenced the Aβ, total tau, and p-tau levels in the AD spectrum.

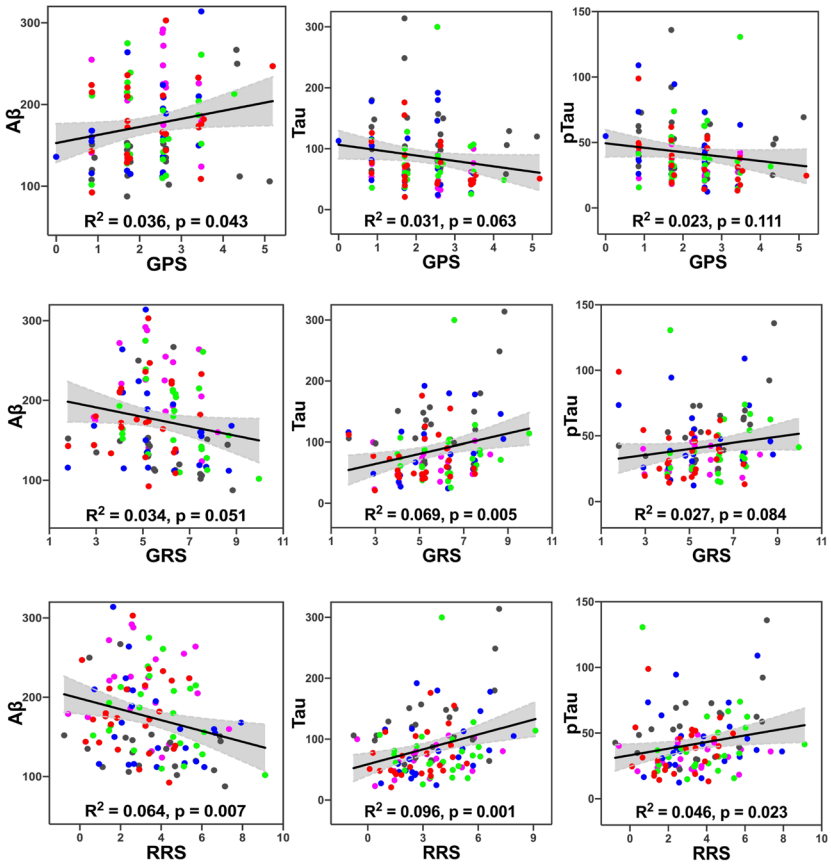

B: Significant linear correlations were found between several lipid metabolism–related markers and total tau but not Aβ and p-tau levels of cerebrospinal fluid in the AD spectrum.

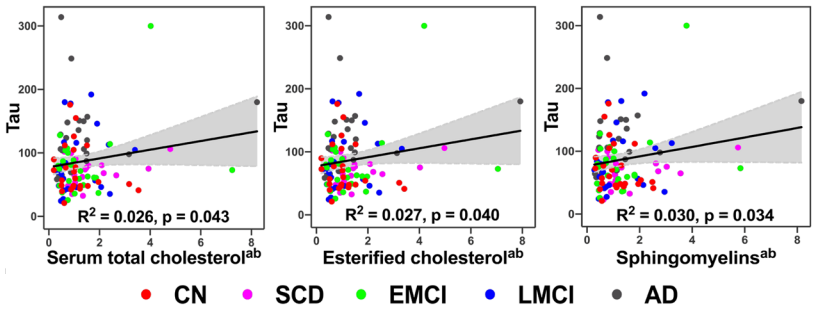

(continued)

performance across all data, linear and binomial nonlinear regression analyses were employed after controlling for covariates of age, sex, education, and APOE ε4 status.

Functional connectivity analysis. Multivariable linear regression analyses were conducted to investigate the main effects of the PGS, and PGS × disease interactive effects on the DMN, controlling for nuisance covariates including age, sex, and education if necessary (3dRegAna, AFNI). Statistical threshold was set at $P < .05$ (3dClustSim corrected with the -acf function, cluster size > 2,727 mm^3 corresponding to cluster $\alpha < .05$, https://afni.nimh.nih.gov/pub/dist/doc/program_help/3dClustSim.html).

The equation of multivariable linear regression analyses was as follows:

$$mi = \beta0 + \beta1 \times dis + \beta2 \times PGS + \beta3 \times (PGS \times dis) + \beta4 \times Age + \beta5 \times Sex + \beta6 \times Edu + \varepsilon$$

Here mi is the *z* value of the functional connectivity (FC) of the ith voxel within DMN across all subjects. β0 is the

Figure 1 (continued).

C: Nonlinear correlations were found between lipid metabolites and ADAS-cog scores.

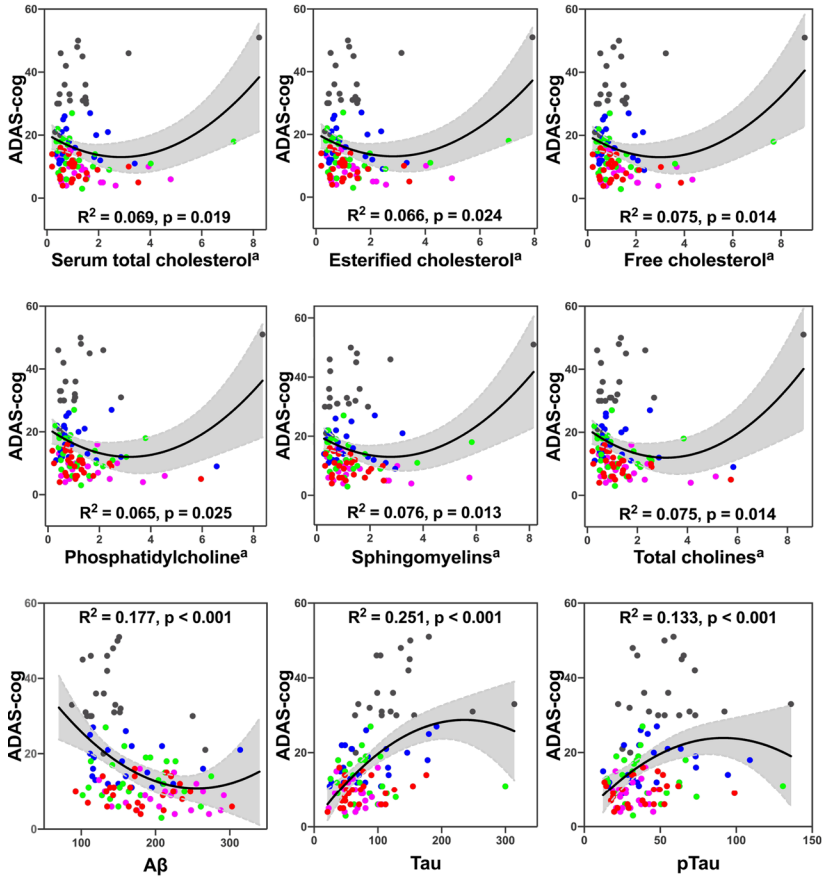

D: Nonlinear curves fitted between cerebrospinal fluid biomarkers and MMSE scores.

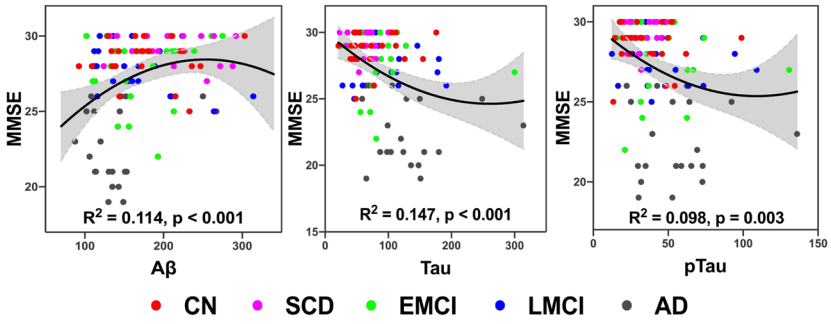

[a]For simplifying the calculation of various indicators, all data for lipids were standardized to facilitate data normally distributed transformed with the formula $z = (x - \mu)/\sigma$, for which x was the specific value, μ was the mean value, and σ the standard deviation. Then, the *z* values of lipids were transformed using an inverse logarithm algorithm with a base of 2. Considering the opposite effects of HDL compared with LDL or VLDL, the values of HDL-related markers were further converted into their reciprocal form.

[b]One-tailed *P* values < .05 were considered significant only in Figure 1B.

*Gray bands indicated 95% confidence intervals.

Abbreviations: Aβ = amyloid β peptides 1 to 42, AD = Alzheimer's disease, ADAS-cog = Alzheimer's Disease Assessment Scale–13-item cognitive subscale, CN = cognitively normal, EMCI = early amnestic mild cognitive impairment, GPS = genetic protective score, GRS = genetic risk score, HDL = high-density lipoprotein, LDL = low-density lipoprotein, LMCI = late mild cognitive impairment, MMSE = Mini-Mental State Examination, p-tau = tau phosphorylated at the threonine-181 position, RRS = relative risk score, SCD = subjective cognitive decline, VLDL = very low density lipoprotein.

Figure 2. Main Effect of Polygenic Scores on the Default Mode Network Across the AD Spectrum[a]

A, E, and I: Brain regions depicting the main effects of GPS, GRS, and RRS on the anterior DMN.

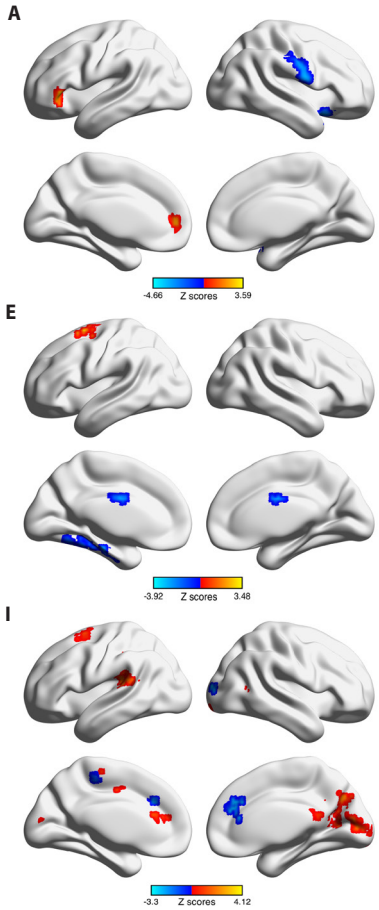

B, F, and J: Representative brain regions with significant correlations between the GPS, GRS, and RRS, respectively, with averaged functional connectivity of the anterior DMN.

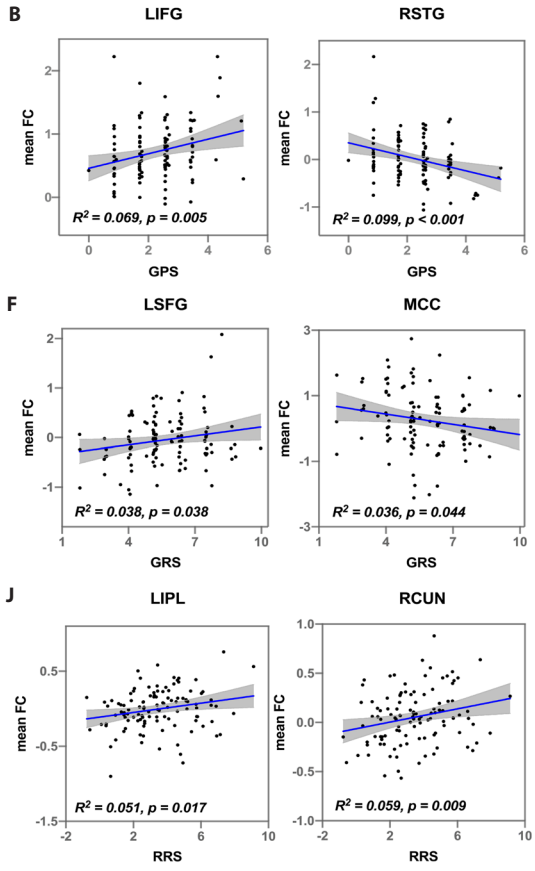

(continued)

intercept of the line fitted in the model. β1, β2, and β3 are the effects of disease, PGS and PGS × disease interaction on the FC strength of the ith voxel in the DMN. β4, β5, and β6 are the main effects of age, sex, and education, respectively, which were discarded as covariates of no interest in the above linear regression model. The error term ε is assumed to be Gaussian distributed and uncorrelated across all subjects.

Next, to investigate the brain maps of lipid metabolites associated with aDMN and pDMN among all data, partial correlation analyses were applied after removing covariates of age, sex, education, and *APOE* ε4 status.

RESULTS

Demographic, Neuropsychological, Genetic, and Molecular Biomarkers

No significant differences were found in age, sex, education, any candidate genotypes except *APOE*, or the lipid metabolites among all participants (all *P* values > .05). Significant group differences existed in cognitive scores and CSF biomarker levels. However, compared with the CN group, only Aβ level was identified as a significant discrepancy in the SCD group. As the disease progressed beyond the stage of SCD, there was a gradually declining trend in MMSE scores and Aβ levels and an increasing trend in ADAS-cog scores, t-tau levels, and p-tau levels. More details were shown in Table 1.

Relationships Between Pairs of PGSs, Lipid Metabolites, CSF Biomarkers, and Cognitive Performance

First, linear regression between PGS and CSF biomarkers revealed that GPS was correlated with Aβ level ($P = .043$) but not t-tau and p-tau levels; in contrast, GRS was correlated with t-tau levels ($P = .005$) and marginally associated with Aβ level ($P = .051$) but not with p-tau level, while RRS was significantly influenced by Aβ ($P = .007$), t-tau ($P = .001$), and p-tau ($P = .023$) levels across the AD spectrum. On removing *APOE* from the lipid pathway, these associations became nonsignificant (data not presented). Several lipid metabolism–related markers, including serum total cholesterol (SERUM_C), esterified cholesterol (EC), and sphingomyelins (SM), were also found to be correlated with

Figure 2 (continued).

C, G, and K: Brain regions showing the main effects of the GPS, GRS, and RRS, respectively, on the posterior DMN.

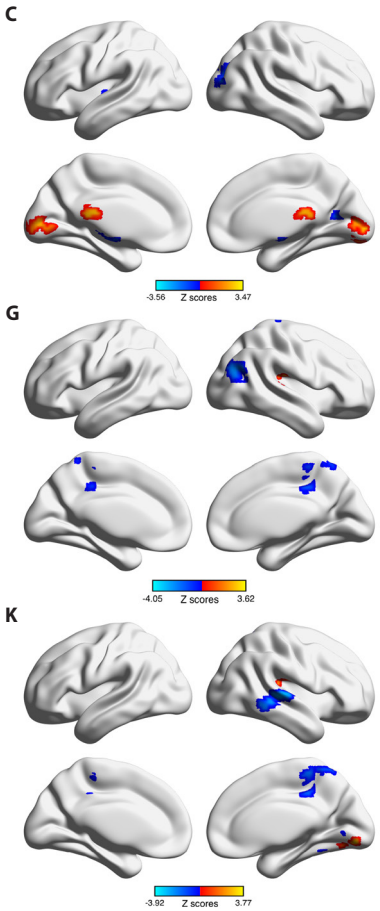

D, H, and L: Representative brain regions with significant correlations between the GPS, GRS, and RRS with averaged functional connectivity of the posterior DMN.

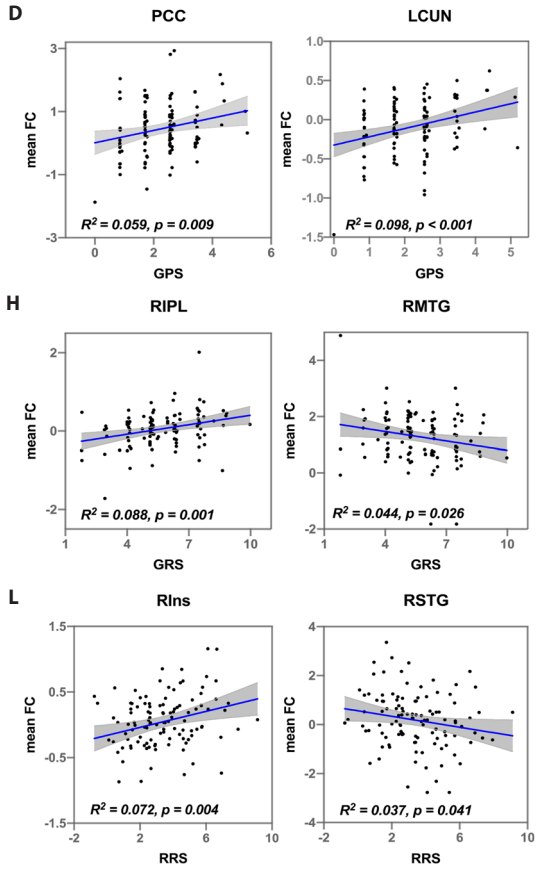

[a]A red color indicates a positive correlation, and a blue color indicates a negative correlation between polygenic scores and functional connectivity strength of the DMN. The color bar indicates *z* scores.

Abbreviations: AD = Alzheimer's disease, DMN = default mode network, FC = functional connectivity, GPS = genetic protective score, GRS = genetic risk score, LCUN = left cuneus, LIFG = left inferior frontal gyrus, LIPL = left inferior parietal lobule, LSFG = left superior frontal gyrus, MCC = middle cingulate cortex, PCC = posterior cingulate cortex, RCUN = right cuneus, RIns = right insula, RIPL = right inferior parietal lobule, RMTG = right middle temporal gyrus, RRS = relative risk score.

t-tau level but not Aβ and p-tau levels in the AD spectrum. Additionally, binomial nonlinear correlations were discovered between several lipid metabolites and ADAS-cog scores but not MMSE scores. These metabolites included SERUM C, EC, free cholesterol (Free Cho), phosphatidylcholine (PC), SM, and total cholines (TOTCHO). Finally, regression analysis disclosed that CSF biomarkers could significantly impact cognitive performance in a nonlinear manner. The aforementioned results are plotted in Figure 1.

Main Effect of PGSs and Interactive Effects of PGSs by Disease on the aDMN and pDMN

Polygenic effects on the subnetworks of DMN were distinct, with effect on the aDMN mostly evident within the frontal cortex (9 of 23 regions), limbic lobe (4/23), and parietal cortex (3/23) and on the pDMN in the temporal cortex (6/19), occipital cortex (4/19), and limbic lobe (4/19). These brain lobes were divided according to human atlas based on connectional architecture.[35] Next, representative brain regions with significant correlations between PGSs and FCs within DMN are presented in Figure 2. These linear correlation graphs depicted the trajectory of FC with the accumulation of PGSs.

Interactive effects of PGSs and disease on the aDMN were principally found in the frontal cortex (6 of 16 regions), temporal cortex (5/16), parietal cortex (1/16), subcortical nuclei (1/16), limbic lobe (2/16), and insular lobe (1/16), and effects on the pDMN were mostly discovered in the temporal cortex (7/19), occipital cortex (3/19), subcortical nuclei (5/19), frontal cortex (1/19), and limbic lobe (3/19). Furthermore, representative brain regions with significant interactive effects are depicted with line charts in Figure 3.

As the disease progressed, FC of typical regions within aDMN presented a declining trajectory; conversely, regarding interactions with pDMN, the FC decreased first and then reached equilibrium with the initial stage of the

Figure 3. Interactive Effects Between Polygenic Scores and Disease on the Default Mode Network Across the AD Spectrum[a]

A, E, and I: Interactive effects between the GPS, GRS, and RRS, respectively, and disease on the anterior DMN in the AD spectrum.

B, F, and J: Linear trends depicted by line charts represent the significant interactive effects of the GPS, GRS, and RRS, respectively, and disease on the anterior DMN in the AD spectrum.

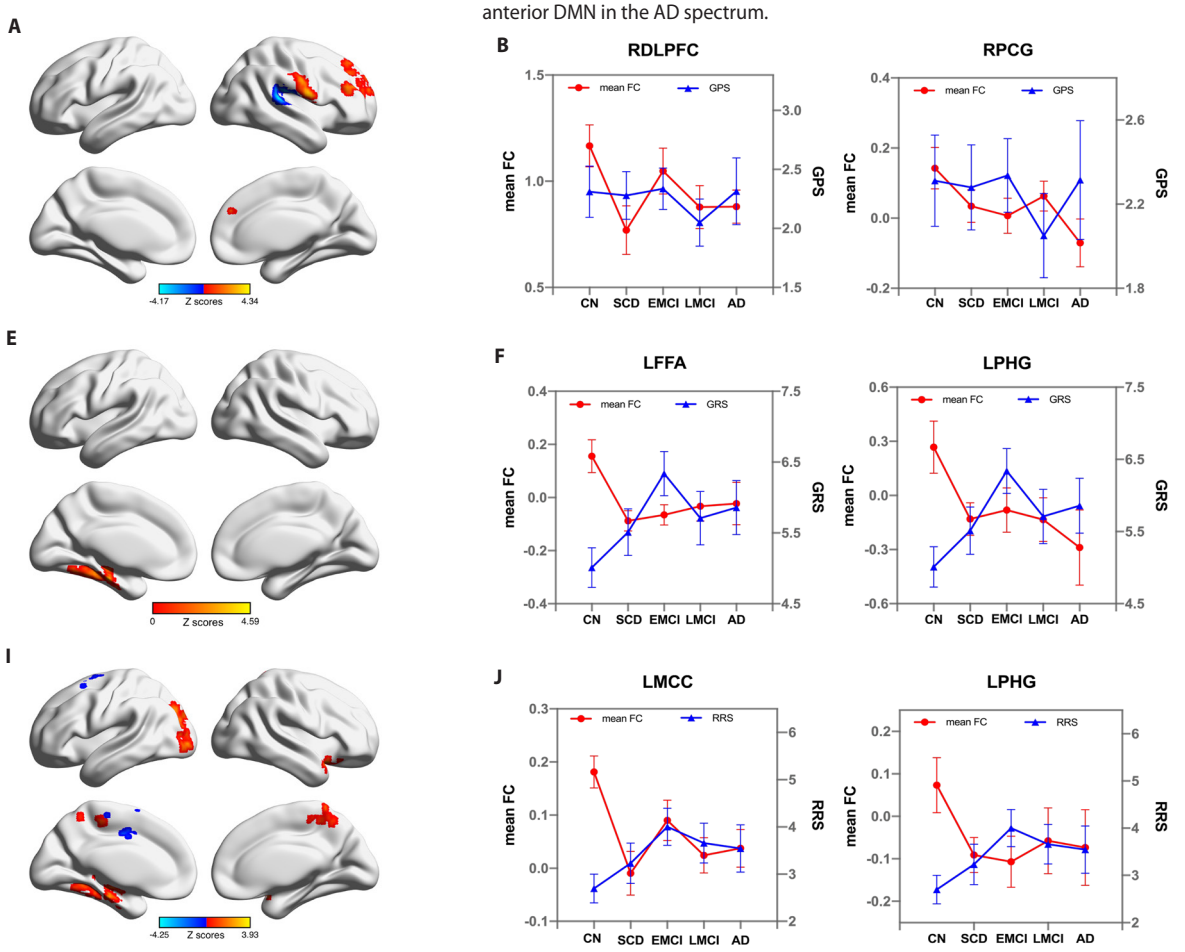

(continued)

CN group. The PGS first increased and then decreased as the disease progressed, with the highest point presenting at the EMCI stage. EMCI patients with higher genetic scores showed weaker FC strength, while patients in other groups with lower genetic scores showed greater FC strength. Negative correlations between the PGS and FC within aDMN were mainly distributed in the left middle cingulate cortex (LMCC), right middle frontal gyrus (RMFG), and left putamen (LPut), and within pDMN, negative correlations were primarily found in the right lingual gyrus (RLG), right parahippocampal gyrus (RPHG), and anterior cingulate cortex (ACC), whereas the PGS was positively correlated with FC in the other brain regions of interactive effects.

Brain Maps of Serum Lipids Correlated With aDMN and pDMN

We found 6 lipid metabolites associated with cognitive performance, and brain regions linked to these lipids were also delineated. These brain regions were involved in the sensorimotor network and occipital lobe, including postcentral gyrus (PCG), supplementary motor area (SMA), posterior cingulate cortex (PCC), and middle occipital gyrus (MOG). Regions related to the aDMN included the right MOG (RMOG), right PCG (RPCG), and SMA, and the regions related to the pDMN included the right PCC (RPCC), left MOG (LMOG), and RPCG. The elevated levels of lipid metabolites were prone to be associated with higher FC in the RMOG, SMA, and PCC but were associated with lower FC in the LMOG and RPCG (for details, see Figure 4).

DISCUSSION

In this study, we proved that the lipid metabolic pathway-specific polygenes could affect the DMN subnetworks and global cognitive performance. The genetic protective, risk, and relative risk scores impacted DMN subsystems in a diverse trajectory across the AD spectrum. These results deepen our knowledge of lipid metabolism affecting the neural system and provide several sensitive lipid indicators to monitor the impairments of lipid metabolism in the brain.

Figure 3 (continued).

C, G, and K: Interactive effects between the GPS, GRS, RRS, and disease, respectively, on the posterior DMN in the AD spectrum.

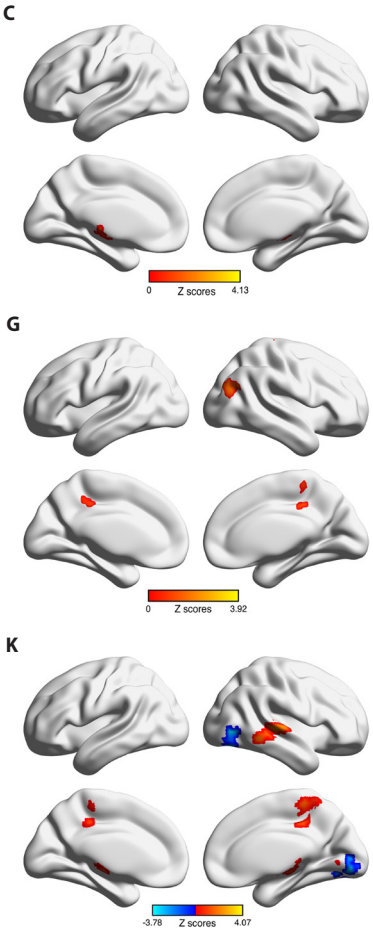

D, H, and L: Linear trends depicted by line charts represent the significant interactive effects of the GPS, GRS, RRS, and disease, respectively, on the posterior DMN in the AD spectrum.

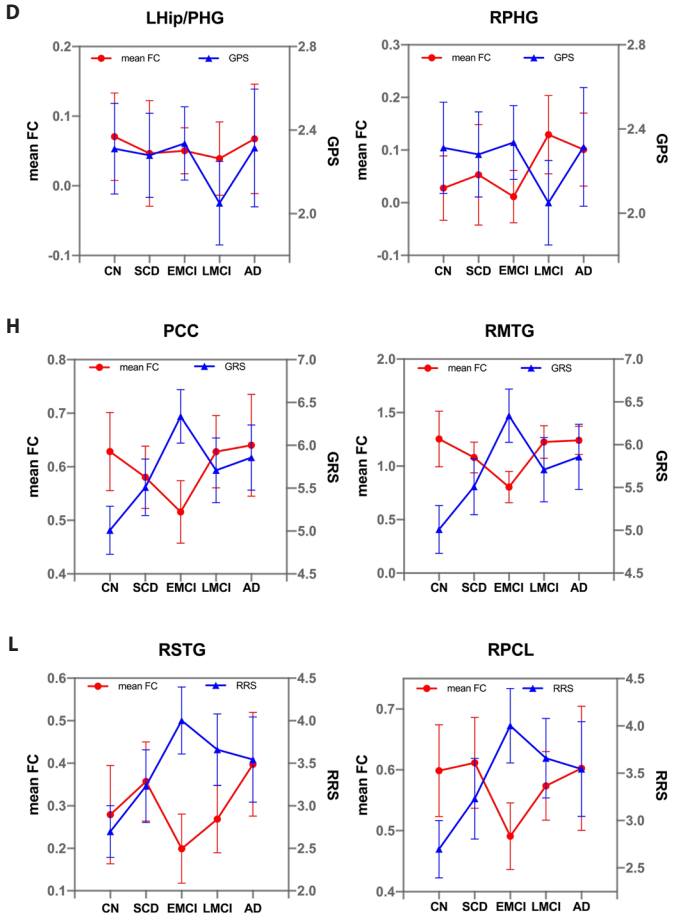

[a]A bright color indicates a positive correlation, and a blue color indicates a negative correlation between polygenic scores and functional connectivity strength of the DMN. The color bar indicates *z* scores.

Abbreviations: AD = Alzheimer's disease, CN = cognitively normal, DMN = default mode network, EMCI = early amnestic mild cognitive impairment, FC = functional connectivity, GPS = genetic protective score, GRS = genetic risk score, LFFA = left fusiform area, LHip/PHG = left hippocampus/parahippocampal gyrus, LMCC = left middle cingulate cortex, LMCI = late mild cognitive impairment, LPHG = left parahippocampal gyrus, PCC = posterior cingulate cortex, RDLPFC = right dorsolateral prefrontal cortex, RMOG = right middle occipital gyrus, RMTG = right middle temporal gyrus, RPCG = right precentral gyrus, RPCL = right paracentral lobule, RPHG = right parahippocampal gyrus, RRS = relative risk score, RSTG = right superior temporal gyrus, SCD = subjective cognitive decline.

The associations between GRS and CSF core biomarkers suggested that a higher GRS was not associated with lower levels of Aβ and higher levels of p-tau; although there was an association with t-tau levels ($P = .005$), on removal of *APOE* from GRS, statistical significance was eliminated. This result indicated that the overall GRS appeared to be driven by the inclusion of a strong *APOE* effect, and the other variants did not add much predictive power. Previously, AD patients with the *APOE* ε4 allele showed increased Aβ plaque deposition and neurofibrillary tangles; in contrast, the presence of *APOE* ε2 might slow the progression of AD pathology.[36] Overall, *APOE* remains a key risk factor for AD pathological changes. We also found that a higher GPS was marginally correlated with higher levels of Aβ but not t-tau and p-tau; after deducting protective factors, a higher RRS was extraordinarily associated with a lower level of Aβ and higher levels of t-tau and p-tau, which hinted at the necessity of distinguishing risk from protective genetic scores. The aforementioned findings were consistent with those from previous studies suggesting that genetic factors of lipid metabolism contributed to pathological changes in AD,[13] with pathway-specific RRS being more predictive than GRS.

In addition, higher levels of SERUM C, EC, and SM were connected with high levels of t-tau, indicating that serum lipids also contribute to tau pathology in AD. However, previous studies showed that cholesterol retention was responsible for Aβ production,[8] and cholesterol depletion reduced aggregation of insoluble Aβ in hippocampal neurons.[37] It is necessary to further verify the relationship between blood lipids and Aβ pathology.

Furthermore, a nonlinear relationship was found between serum or CSF molecular biomarkers and general cognitive

Figure 4. Brain Maps of Lipid Metabolites Associated With the Anterior and Posterior Default Mode Network[a]

A, E, I, M, Q, and U: Brain maps of total serum cholesterol, esterified cholesterol, free cholesterol, phosphatidylcholine, sphingomyelins, and total cholines, respectively, correlated with the anterior DMN.

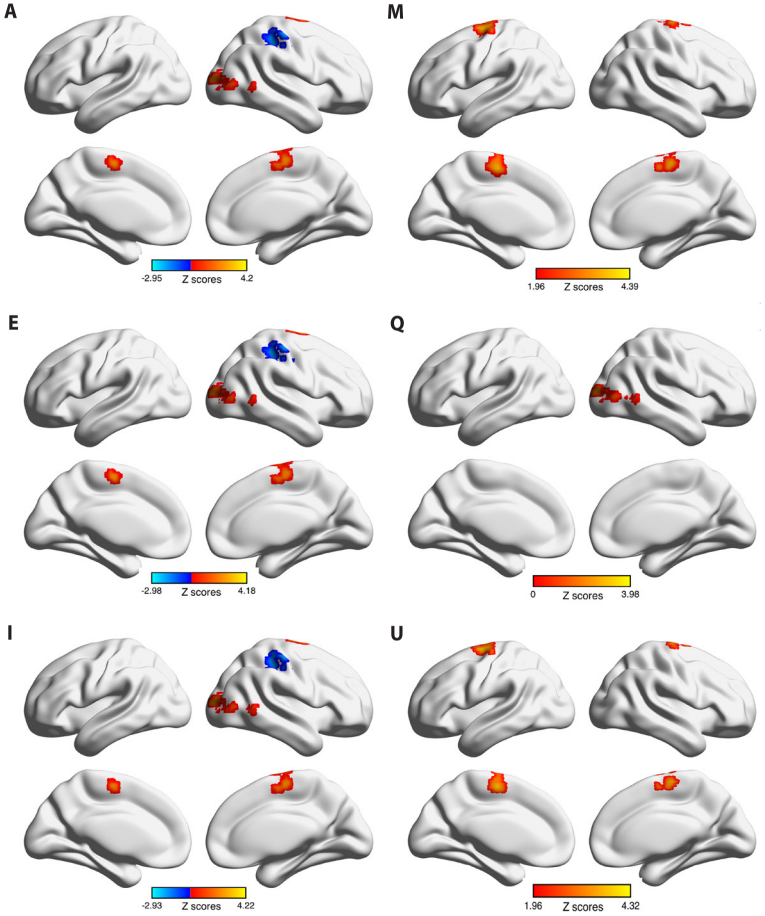

B, F, J, N, R and V: Linear correlation charts of representative regions stemming from the anterior DMN.

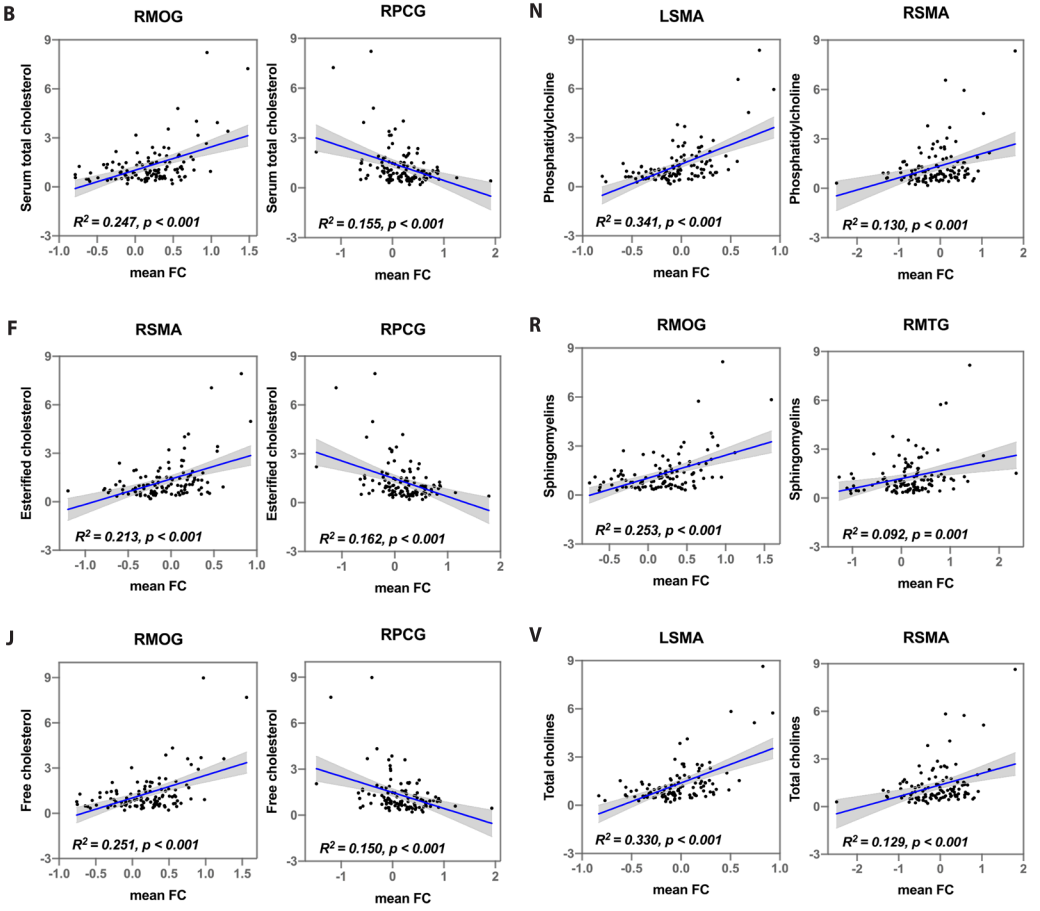

(continued)

Figure 4. (continued)

C, G, K, O, S and W: Brain maps of total serum cholesterol, esterified cholesterol, free cholesterol, phosphatidylcholine, sphingomyelins, and total cholines, respectively, correlated with the posterior DMN.

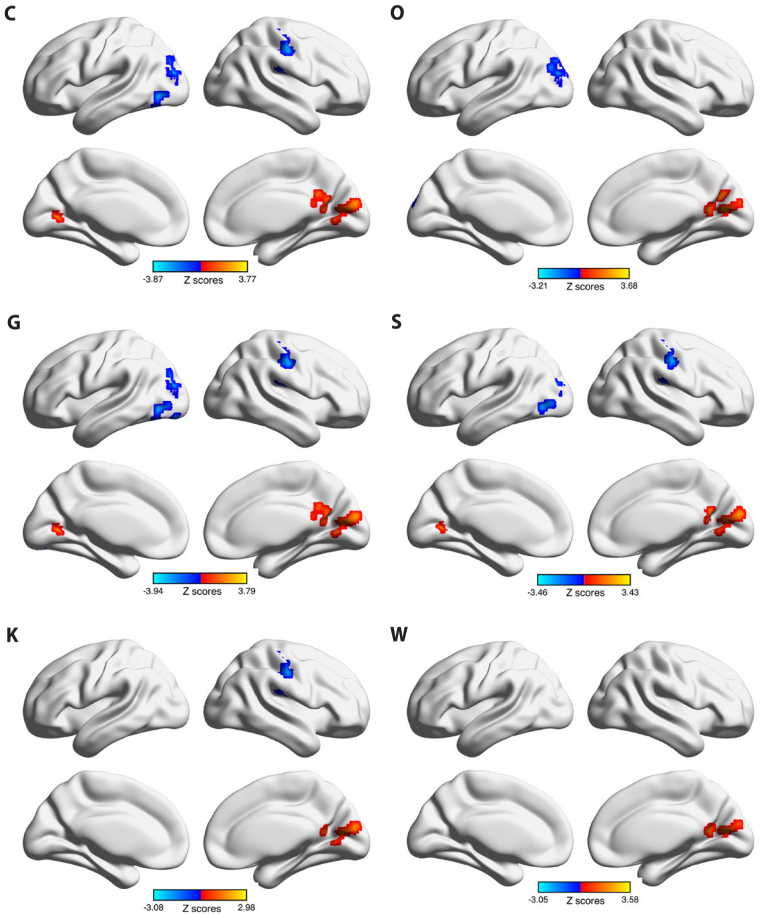

D, H, L, P, T and X: Linear correlation charts of representative regions extracted from the posterior DMN.

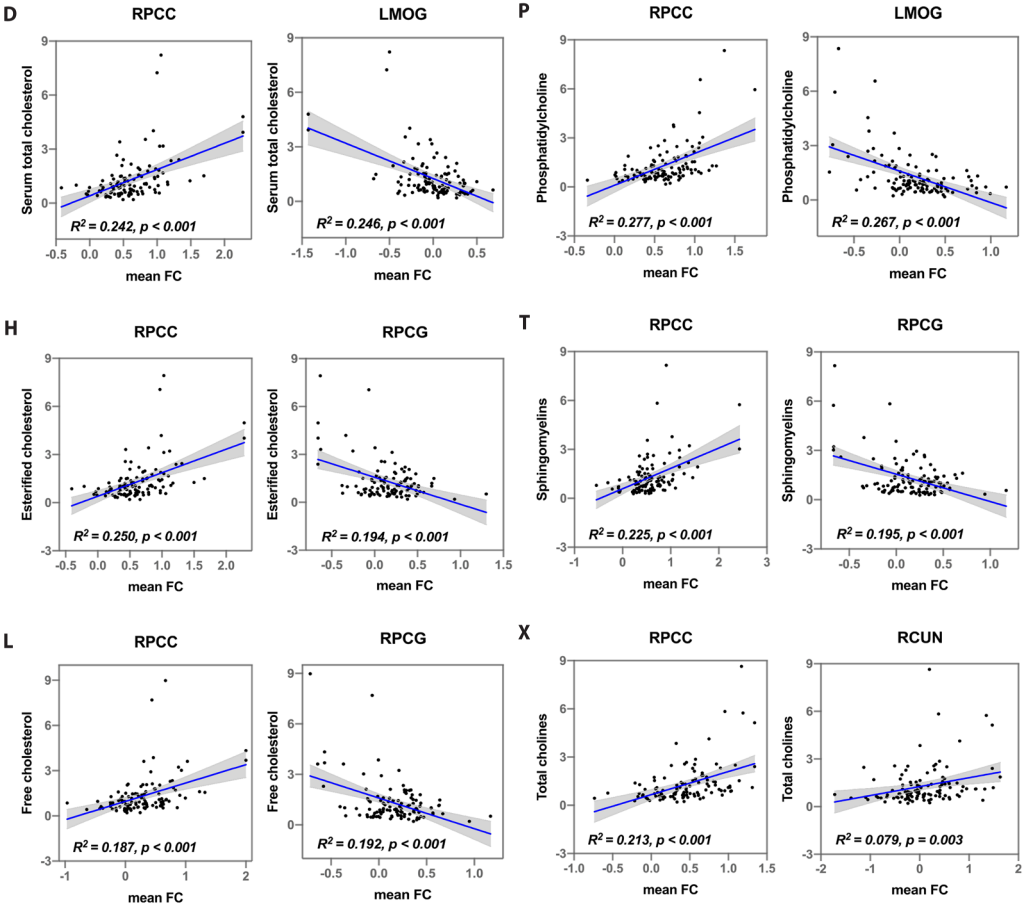

[a]A bright color indicates lipid metabolites positively correlated with the anterior DMN, and a blue color indicates a negative correlation between them. The color bar indicates *z* scores.

Abbreviations: DMN = default mode network, FC = functional connectivity, LMOG = left middle occipital gyrus, LSMA = left supplementary motor area, RCUN = right cuneus, RMOG = right middle occipital gyrus, RMTG = right middle temporal gyrus, RPCC = left posterior cingulate cortex, RPCG = right precentral gyrus, RSMA = right supplementary motor area.

performance. These biomarkers include SERUM_C, EC, Free Cho, PC, SM, and TOTCHO, all of which are prominent structural and physiologic constituents of neural biofilms in the brain. The nonlinear related curve between lipids and cognitive score shows the first decline and then upward trend, indicating that higher serum lipids are beneficial to the elderly and may promote cognition, while lower lipid levels may aggravate cognitive impairment, which is consistent with previous studies.[38,39] This result also reminds us of the importance of monitoring serum lipids at early stages of AD. The relationship between CSF biomarkers and cognition has been extensively investigated.[40–43] The curved relationship was more consistent with the accelerated cognitive decline exhibited across the disease process.[44] This finding may offer several sensitive lipid indicators to monitor cognitive impairments and provide specific targets for improving cognition by lipid-lowering therapy.

The extensive effects across DMN subsystems differed at different stages along the AD spectrum. This distributional discrepancy is mainly because the DMN subsystems have distinct anatomic, functional, and pathophysiologic profiles.[20,45,46] The medial prefrontal cortex and PCC, revealed as prominent core hubs of the aDMN and pDMN, also have different functional divisions,[47] with the former hub related to social cognition[48] and the latter playing a central role in autobiographical memory retrieval and planning for the future.[49]

Additionally, brain regions of broad genetic and interactive effects were largely concentrated in the cortical frontal-parietal network and subcortical basal ganglia network, which have been deemed to underlie rhythmic spatial attention[50] and inhibitory control of action and cognition.[51,52] Also, the accumulated genetic distribution indicated that brain areas positively correlated with PGS (in the same direction) might play a major compensatory role in disease progression, while those areas in the opposite direction (negatively correlated) might have been decompensated and destroyed. However, the impact of polygenes on FC changes was not strong, with most R^2 values being less than 10%. This might be explained by the fact that FC could compensate for cognitive decline in cognitively normal individuals, while decompensation occurred in prodromal AD stages.[53,54] The overall contributions of FC were weakened across the AD spectrum.

Furthermore, the interplay relationship of polygenes and disease facilitated PGS and FC, presenting changing trajectory as the disease progressed. The declining tendency and inverse U-shaped pattern of FC have been reported by previous studies.[55] The PGSs changed, first increasing and then decreasing, with the highest score in the EMCI stage. Notably, we found decreased FC in EMCI patients and increased FC in subjects from other groups. Bound by the EMCI stage, these opposite trajectory changes within DMN across AD spectrum might be attributed to different neural mechanisms underlying AD progression. As the individuals with SCD will not show a cognitive decline,[56] the EMCI stage has become the earliest symptomatic stage with worse cognitive performance.[57] Thus, following up recruiting of SCD patients in a timely manner is of vital importance for clinical intervention and disease prognosis.

Previous lipid-related imaging studies have revealed the effects of lipids on the brain.[14–17] We also discovered specific brain regions associated with serum lipids that are mainly involved in the sensorimotor network and regions of the PCC and MOG. Earlier studies suggested that youth at risk for obesity showed elevated reward circuitry responsivity coupled with elevated responsivity to food in somatosensory regions, and the latter might lead to overeating, consequently producing blunted dopamine signaling and elevated responsivity to food cues.[58] In individuals with high body mass index values, females showed greater centrality in reward (amygdala, hippocampus) and salience (anterior midcingulate cortex) regions than males.[59] Moreover, another study with a 6-month exercise program in obese individuals[60] showed that exercise could affect communications between networks to enhance individual responsivity to exercise, especially for the PCC, with reductions in both outgoing and ingoing causal flow to several resting networks. The present study effectively combined lipid profile, brain network, and cognition, providing a brain atlas of cognitively related lipid profiles for future studies. Naturally, differences existed in the brain regions related to aDMN and pDMN, which also proved that there was divergence within the effects of lipid metabolism on the DMN. It was evident that the aDMN linked more to posterior components with the FFA, cingulate cortex, or precuneus and the pDMN was inclined to connect with the prefrontal and parietal cortex. This anterior-posterior functional coupling across the AD continuum might lead to opposing roles for the DMN subnetworks on cognitive impairment.

Several limitations remain in this study. First, due to the limited fMRI data in the ADNI database, the study sample is small, and it is necessary to replicate and validate these results in a larger sample. Second, although the selected genes do not belong to a specific single pathway, their eponymous proteins are involved in biological processes related to lipid metabolism. Then, these genes are considered to be in the lipid metabolic pathway. However, the number of genetic loci included in the ADNI database is limited. As more genetic loci are covered in the public database, further studies need to increase the number of loci to enrich the lipid pathway. Third, this study investigated the polygenic effects on DMN only; thus, how lipid-related polygenes impact other functional networks was unclear. It is worth researching the polygenic effect on the other networks. Fourth, although the methodology was not thorough, with no adjustment for multiple testing, several key molecular biomarkers were selected from a variety of lipid metabolites that showed the most relevant trend to cognition. Finally, the brain regions associated with serum lipids were in the sensorimotor network and occipital lobule. Targeted therapy, especially physical stimulation therapy, on the cortical supplementary motor area region may reduce lipid levels and further improve cognitive function.

Submitted: November 2, 2020; accepted April 15, 2021.

Published online: September 21, 2021.

Potential conflicts of interest: None.

Funding/support: This study was granted funding by the National Key Projects for Research and Development Program of China (2016YFC1305800, 2016YFC1305802, CMX), the National Natural Science Foundation of China (81671256, 81871069, CMX), the Key Project for Research and Development Program of Jiangsu Province (BE2018741), the Nanjing International Joint Research and Development Project (201715013), the Postgraduate Research & Practice Innovation Program of Jiangsu Province (KYCX19_0115), the Alzheimer's Disease Neuroimaging Initiative (ADNI) (National Institutes of Health Grant U01 AG024904), and the Alzheimer's Disease Metabolomics Consortium (National Institute on Aging R01AG046171, RF1AG051550 and 3U01AG024904-09S4).

Role of the sponsor: Data collection was funded by the Alzheimer's Disease Neuroimaging Initiative (ADNI) and the Alzheimer's Disease Metabolomics Consortium. The other sponsors provided financial support for data analysis and editorial support in the publication of this article.

Additional information: The data used in preparation of this article were obtained from the Alzheimer's disease Neuroimaging Initiative (ADNI) database (http://adni.loni.usc.edu/). Investigators within the ADNI database contributed to the design and implementation of the ADNI and provided data but did not participate in the analysis or write this report. For a complete listing of ADNI investigators, please see http://adni.loni.usc.edu/wp-content/uploads/how_to_apply/ADNI_Acknowledgement_List.pdf. The plasma lipid data used in this article were generated by the Alzheimer's Disease Metabolomics Consortium (ADMC) and delivered by the ADNI website. A complete listing of ADMC investigators can be found at https://sites.duke.edu/adnimetab/team/.

Supplementary material: Available at PSYCHIATRIST.COM.

REFERENCES

1. Refolo LM, Malester B, LaFrancois J, et al. Hypercholesterolemia accelerates the Alzheimer's amyloid pathology in a transgenic mouse model. *Neurobiol Dis*. 2000;7(4):321–331.
2. Luo R, Su LY, Li G, et al. Activation of PPARA-mediated autophagy reduces Alzheimer disease-like pathology and cognitive decline in a murine model. *Autophagy*. 2020;16(1):52–69.
3. Whitmer RA, Gunderson EP, Barrett-Connor E, et al. Obesity in middle age and future risk of dementia: a 27 year longitudinal population based study. *BMJ*. 2005;330(7504):1360.
4. Proitsi P, Lupton MK, Velayudhan L, et al; Alzheimer's Disease Neuroimaging Initiative; GERAD1 Consortium. Genetic predisposition to increased blood cholesterol and triglyceride lipid levels and risk of Alzheimer disease: a Mendelian randomization analysis. *PLoS Med*. 2014;11(9):e1001713.
5. Cutler RG, Kelly J, Storie K, et al. Involvement of oxidative stress-induced abnormalities in ceramide and cholesterol metabolism in brain aging and Alzheimer's disease. *Proc Natl Acad Sci U S A*. 2004;101(7):2070–2075.
6. Leduc V, Jasmin-Bélanger S, Poirier J. APOE and cholesterol homeostasis in Alzheimer's disease. *Trends Mol Med*. 2010;16(10):469–477.
7. Ehehalt R, Keller P, Haass C, et al. Amyloidogenic processing of the Alzheimer beta-amyloid precursor protein depends on lipid rafts. *J Cell Biol*. 2003;160(1):113–123.
8. Xiong H, Callaghan D, Jones A, et al. Cholesterol retention in Alzheimer's brain is responsible for high beta- and gamma-secretase activities and Abeta production. *Neurobiol Dis*. 2008;29(3):422–437.
9. Götz J, Chen F, van Dorpe J, et al. Formation of neurofibrillary tangles in P301l tau transgenic mice induced by Abeta 42 fibrils. *Science*. 2001;293(5534):1491–1495.
10. van der Kant R, Goldstein LSB, Ossenkoppele R. Amyloid-β-independent regulators of tau pathology in Alzheimer disease. *Nat Rev Neurosci*. 2020;21(1):21–35.
11. Popp J, Meichsner S, Kölsch H, et al. Cerebral and extracerebral cholesterol metabolism and CSF markers of Alzheimer's disease. *Biochem Pharmacol*. 2013;86(1):37–42.
12. Wong MW, Braidy N, Poljak A, et al. Dysregulation of lipids in Alzheimer's disease and their role as potential biomarkers. *Alzheimers Dement*. 2017;13(7):810–827.
13. Darst BF, Koscik RL, Racine AM, et al. Pathway-specific polygenic risk scores as predictors of amyloid-β deposition and cognitive function in a sample at increased risk for Alzheimer's disease. *J Alzheimers Dis*. 2017;55(2):473–484.
14. Koschack J, Lütjohann D, Schmidt-Samoa C, et al. Serum 24S-hydroxycholesterol and hippocampal size in middle-aged normal individuals. *Neurobiol Aging*. 2009;30(6):898–902.
15. Zhang T, Li H, Zhang J, et al. Impacts of high serum total cholesterol level on brain functional connectivity in non-demented elderly. *J Alzheimers Dis*. 2016;50(2):455–463.
16. Moazzami K, Power MC, Gottesman R, et al. Association of mid-life serum lipid levels with late-life brain volumes: the atherosclerosis risk in communities neurocognitive study (ARICNCS). *Neuroimage*. 2020;223:117324.
17. Iriondo A, García-Sebastian M, Arrospide A, et al. Plasma lipids are associated with white matter microstructural changes and axonal degeneration. *Brain Imaging Behav*. 2021;15(2):1043–1057.
18. Qin P, Liu Y, Shi J, et al. Dissociation between anterior and posterior cortical regions during self-specificity and familiarity: a combined fMRI-meta-analytic study. *Hum Brain Mapp*. 2012;33(1):154–164.
19. Leech R, Kamourieh S, Beckmann CF, et al. Fractionating the default mode network: distinct contributions of the ventral and dorsal posterior cingulate cortex to cognitive control. *J Neurosci*. 2011;31(9):3217–3224.
20. Jones DT, Knopman DS, Gunter JL, et al; Alzheimer's Disease Neuroimaging Initiative. Cascading network failure across the Alzheimer's disease spectrum. *Brain*. 2016;139(pt 2):547–562.
21. Damoiseaux JS, Prater KE, Miller BL, et al. Functional connectivity tracks clinical deterioration in Alzheimer's disease. *Neurobiol Aging*. 2012;33(4):828.e19–828.e30.
22. Aisen PS, Petersen RC, Donohue M, et al; Alzheimer's Disease Neuroimaging Initiative. Alzheimer's Disease Neuroimaging Initiative 2 clinical core: progress and plans. *Alzheimers Dement*. 2015;11(7):734–739.
23. Harold D, Abraham R, Hollingworth P, et al. Genome-wide association study identifies variants at CLU and PICALM associated with Alzheimer's disease. *Nat Genet*. 2009;41(10):1088–1093.
24. Olgiati P, Politis AM, Papadimitriou GN, et al. Genetics of late-onset Alzheimer's disease: update from the alzgene database and analysis of shared pathways. *Int J Alzheimers Dis*. 2011;2011:832379.
25. Wang Y, Liu S, Wang J, et al. Association between LRP1 C766T polymorphism and Alzheimer's disease susceptibility: a meta-analysis. *Sci Rep*. 2017;7(1):8435.
26. Xiao E, Chen Q, Goldman AL, et al. Late-onset Alzheimer's disease polygenic risk profile score predicts hippocampal function. *Biol Psychiatry Cogn Neurosci Neuroimaging*. 2017;2(8):673–679.
27. Rogaeva E, Meng Y, Lee JH, et al. The neuronal sortilin-related receptor SORL1 is genetically associated with Alzheimer disease. *Nat Genet*. 2007;39(2):168–177.
28. Chen JJ, Li YM, Zou WY, et al. Relationships between CETP genetic polymorphisms and Alzheimer's disease risk: a meta-analysis. *DNA Cell Biol*. 2014;33(11):807–815.
29. Wollmer MA. Cholesterol-related genes in Alzheimer's disease. *Biochim Biophys Acta*. 2010;1801(8):762–773.
30. Hollingworth P, Harold D, Sims R, et al; Alzheimer's Disease Neuroimaging Initiative; CHARGE consortium; EADI1 consortium. Common variants at ABCA7, MS4A6A/MS4A4E, EPHA1, CD33 and CD2AP are associated with Alzheimer's disease. *Nat Genet*. 2011;43(5):429–435.
31. Saykin AJ, Shen L, Foroud TM, et al; Alzheimer's Disease Neuroimaging Initiative. Alzheimer's Disease Neuroimaging Initiative biomarkers as quantitative phenotypes: Genetics core aims, progress, and plans. *Alzheimers Dement*. 2010;6(3):265–273.
32. Ahmad S, Bannister C, van der Lee SJ, et al. Disentangling the biological pathways involved in early features of Alzheimer's disease in the Rotterdam Study. *Alzheimers Dement*. 2018;14(7):848–857.
33. Jia XZ, Wang J, Sun HY, et al. RESTplus: an improved toolkit for resting-state functional magnetic resonance imaging data processing. *Sci Bull (Beijing)*. 2019;64(14):953–954.
34. Kaneko H, Arakawa M, Funatsu K. Development of a new regression analysis method using independent component analysis. *J Chem Inf Model*. 2008;48(3):534–541.
35. Fan L, Li H, Zhuo J, et al. The Human Brainnetome Atlas: a new brain atlas based on connectional architecture. *Cereb Cortex*. 2016;26(8):3508–3526.
36. Nagy Z, Esiri MM, Jobst KA, et al. Influence of the apolipoprotein E genotype on amyloid deposition and neurofibrillary tangle formation in Alzheimer's disease. *Neuroscience*. 1995;69(3):757–761.
37. Schneider A, Schulz-Schaeffer W, Hartmann T, et al. Cholesterol depletion reduces aggregation of amyloid-beta peptide in hippocampal neurons. *Neurobiol Dis*. 2006;23(3):573–577.
38. Reitz C, Tang MX, Luchsinger J, et al. Relation of plasma lipids to Alzheimer disease and vascular dementia. *Arch Neurol*. 2004;61(5):705–714.
39. van den Kommer TN, Dik MG, Comijs HC, et al. Total cholesterol and oxysterols: early markers for cognitive decline in elderly? *Neurobiol Aging*. 2009;30(4):534–545.
40. Hanseeuw BJ, Betensky RA, Jacobs HIL, et al. Association of amyloid and tau with cognition in preclinical Alzheimer disease: a longitudinal study. *JAMA Neurol*. 2019;76(8):915–924.
41. Hansson O, Seibyl J, Stomrud E, et al; Swedish BioFINDER study group; Alzheimer's Disease Neuroimaging Initiative. CSF biomarkers of Alzheimer's disease concord with amyloid-β PET and predict clinical progression: a study of fully automated immunoassays in BioFINDER

and ADNI cohorts. *Alzheimers Dement*. 2018;14(11):1470–1481.
42. Ritchie C, Smailagic N, Noel-Storr AH, et al. CSF tau and the CSF tau/ABeta ratio for the diagnosis of Alzheimer's disease dementia and other dementias in people with mild cognitive impairment (MCI). *Cochrane Database Syst Rev*. 2017;3:CD010803.
43. van der Vlies AE, Verwey NA, Bouwman FH, et al. CSF biomarkers in relationship to cognitive profiles in Alzheimer disease. *Neurology*. 2009;72(12):1056–1061.
44. Mattsson N, Palmqvist S, Stomrud E, et al. Staging β-amyloid pathology with amyloid positron emission tomography. *JAMA Neurol*. 2019;76(11):1319–1329.
45. Jones DT, Machulda MM, Vemuri P, et al. Age-related changes in the default mode network are more advanced in Alzheimer disease. *Neurology*. 2011;77(16):1524–1531.
46. Andrews-Hanna JR, Reidler JS, Sepulcre J, et al. Functional-anatomic fractionation of the brain's default network. *Neuron*. 2010;65(4):550–562.
47. Buckner RL, Andrews-Hanna JR, Schacter DL. The brain's default network: anatomy, function, and relevance to disease. *Ann N Y Acad Sci*. 2008;1124(1):1–38.
48. Amodio DM, Frith CD. Meeting of minds: the medial frontal cortex and social cognition. *Nat Rev Neurosci*. 2006;7(4):268–277.
49. Leech R, Sharp DJ. The role of the posterior cingulate cortex in cognition and disease. *Brain*. 2014;137(pt 1):12–32.
50. Fiebelkorn IC, Pinsk MA, Kastner S. A dynamic interplay within the frontoparietal network underlies rhythmic spatial attention. *Neuron*. 2018;99(4):842–853.e8.
51. Aron AR, Durston S, Eagle DM, et al. Converging evidence for a fronto-basal-ganglia network for inhibitory control of action and cognition. *J Neurosci*. 2007;27(44):11860–11864.
52. Eagle DM, Baunez C, Hutcheson DM, et al. Stop-signal reaction-time task performance: role of prefrontal cortex and subthalamic nucleus. *Cereb Cortex*. 2008;18(1):178–188.
53. Bakker A, Krauss GL, Albert MS, et al. Reduction of hippocampal hyperactivity improves cognition in amnestic mild cognitive impairment. *Neuron*. 2012;74(3):467–474.
54. Qi Z, Wu X, Wang Z, et al. Impairment and compensation coexist in amnestic MCI default mode network. *Neuroimage*. 2010;50(1):48–55.
55. Ye Q, Chen H, Su F, et al. An inverse u-shaped curve of resting-state networks in individuals at high risk of Alzheimer's disease. *J Clin Psychiatry*. 2018;79(2):17m11583.
56. Jessen F, Amariglio RE, Buckley RF, et al. The characterisation of subjective cognitive decline. *Lancet Neurol*. 2020;19(3):271–278.
57. Aisen PS, Petersen RC, Donohue MC, et al; Alzheimer's Disease Neuroimaging Initiative. Clinical core of the Alzheimer's Disease Neuroimaging Initiative: progress and plans. *Alzheimers Dement*. 2010;6(3):239–246.
58. Stice E, Yokum S, Burger KS, et al. Youth at risk for obesity show greater activation of striatal and somatosensory regions to food. *J Neurosci*. 2011;31(12):4360–4366.
59. Gupta A, Mayer EA, Hamadani K, et al. Sex differences in the influence of body mass index on anatomical architecture of brain networks. *Int J Obes*. 2017;41(8):1185–1195.
60. Legget KT, Wylie KP, Cornier MA, et al. Exercise-related changes in between-network connectivity in overweight/obese adults. *Physiol Behav*. 2016;158:60–67.

Editor's Note: We encourage authors to submit papers for consideration as a part of our Focus on Geriatric Psychiatry section. Please contact Jordan F. Karp, MD, at jkarp@psychiatrist.com, or Gary W. Small, MD, at gsmall@psychiatrist.com.

See supplementary material for this article at PSYCHIATRIST.COM.

THE JOURNAL OF
CLINICAL PSYCHIATRY
THE OFFICIAL JOURNAL OF THE AMERICAN SOCIETY OF CLINICAL PSYCHOPHARMACOLOGY

Supplementary Material

Article Title: Polygenic Effects of the Lipid Metabolic Pathway Accelerated Pathological Changes and Disrupted Default Mode Network Trajectory Across the Alzheimer's Disease Spectrum

Author(s): Feifei Zang, PhD; Yao Zhu, PhD; Xinyi Liu, PhD; Dandan Fan, PhD; Qing Wang, PhD; Qianqian Zhang, MD; Cancan He, PhD; Zhijun Zhang, MD, PhD; and Chunming Xie, MD, PhD, on behalf of Alzheimer's Disease Neuroimaging Initiative and the Alzheimer Disease Metabolomics Consortium

DOI Number: https://doi.org/10.4088/JCP.20m13739

List of Supplementary Material for the article

1. Figure 1 Participant flow
2. Table 1 Summary information of lipid metabolic pathway related multiple genes

Disclaimer

This Supplementary Material has been provided by the author(s) as an enhancement to the published article. It has been approved by peer review; however, it has undergone neither editing nor formatting by in-house editorial staff. The material is presented in the manner supplied by the author.

Supplementary Figure 1. Participant flow

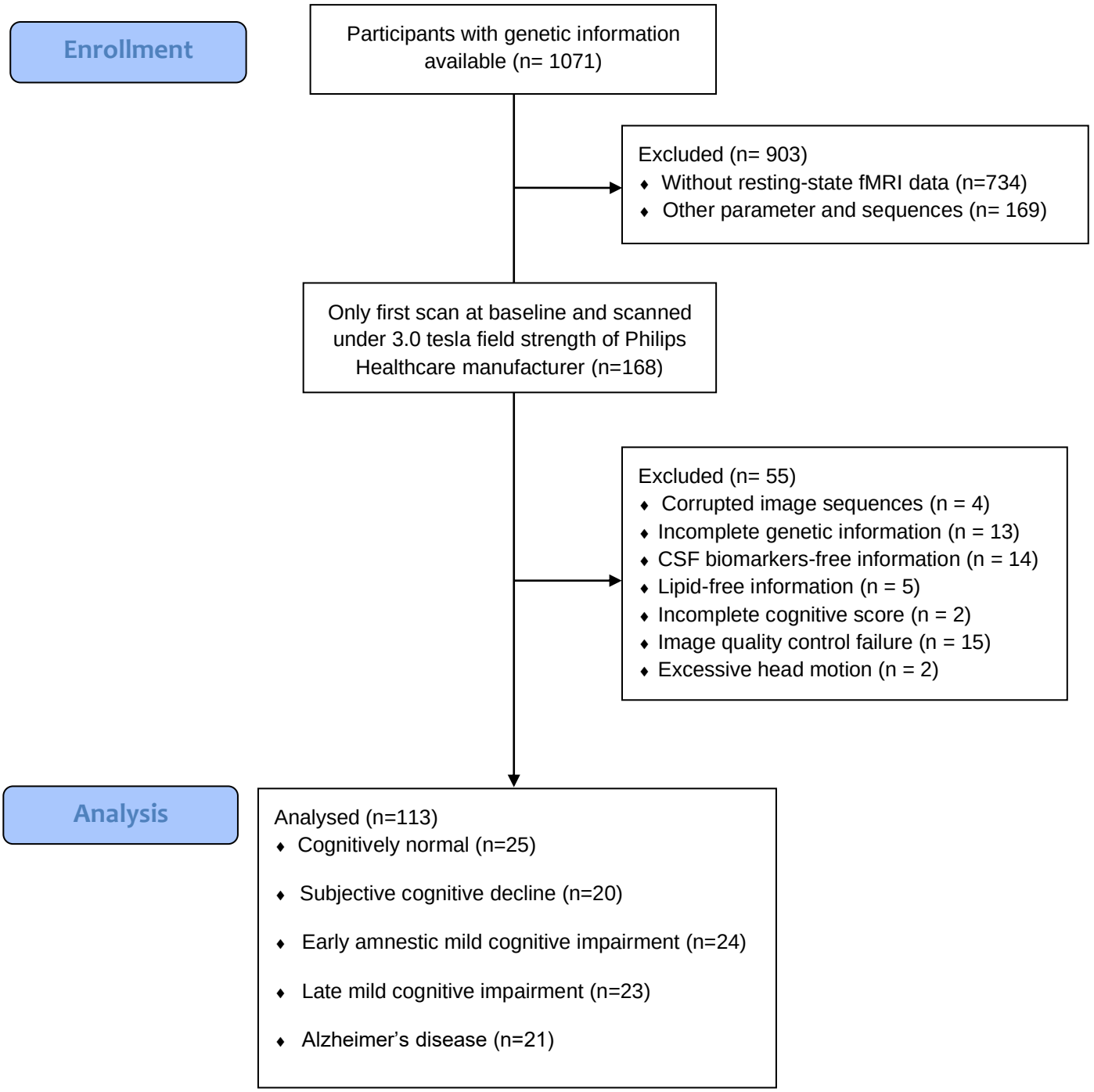

Supplementary Table 1. Summary information of lipid metabolic pathway related multiple genes.

SNP	Chr.	Position	Closest gene	Allele change	GMAF	OR	HWE		Function
							χ^2	p	
rs11136000	8	27607002	CLU	T>C	0.3848	0.86	0.974	0.324	CLU is related to cholesterol reverse transporting.[1]
rs5930	19	11113589	LDLR	A>G	0.3450	0.85	0.071	0.791	Elevated level of LDLR in the brain promotes extracellular Aβ clearance.[2]
rs1799986	12	57141483	LRP1	C>T	0.1047	0.92	0.293	0.588	Blood brain barrier-associated pericytes internalize and clear aggregated Aβ through LRP1-dependent APOE subtype-specific mechanism.[3]
rs3851179	11	86157598	PICALM	T>C	0.3297	0.85	1.440	0.230	PICALM participates in receptor-mediated endocytosis as lipid internalization and transport mediated by lipoprotein particles containing APOE and CLU.[4]
rs2070045	11	121577381	SORL1	T>G	0.3214	1.13	0.381	0.537	SORL1 can bind lipoprotein particles containing APOE and mediate their endocytosis.[5]
rs5882	16	56982180	CETP	G>A	0.4481	1.11	0.043	0.836	CETP mediates the transfer of cholesterol esters from HDL to VLDL, thus promoting the balanced exchange of triglycerides and regulating HDL levels.[6]
rs2230808	9	104800523	ABCA1	T>C	0.4109	1.10	0.870	0.351	ABCA1 regulates APOE levels, lipidation, and APOE-mediated cholesterol transfer from glial cells to neurons.[7]
rs744373	2	127137039	BIN1	A>G	0.3714	1.17	0.227	0.634	BIN1 is also associated with receptor-mediated endocytosis.[8]
rs429358 19 rs7412		45411941 45412079	APOE	- -	- -	- -	1.391	0.238	APOE is a major cholesterol carrier and APOE isoforms differentially regulate Aβ aggregation and clearance in the brain.[9]

Abbreviations: Chr. = chromosome; GMAF = global minor allele frequency reported from 1000Genome genotype data; HWE = Hardy-Weinberg equilibrium; OR = odds ratio for the minor allele; SNP = single nucleotide polymorphism.

Supplementary References

1. Gelissen IC, Hochgrebe T, Wilson MR, et al. Apolipoprotein J (clusterin) induces cholesterol export from macrophage-foam cells: a potential anti-atherogenic function? *The Biochemical journal*. Apr 1 1998;331(Pt 1):231-7.

2. Kim J, Castellano JM, Jiang H, et al. Overexpression of low-density lipoprotein receptor in the brain markedly inhibits amyloid deposition and increases extracellular A beta clearance. *Neuron*. Dec 10 2009;64(5):632-44.

3. Ma Q, Zhao Z, Sagare AP, et al. Blood-brain barrier-associated pericytes internalize and clear aggregated amyloid-β42 by LRP1-dependent apolipoprotein E isoform-specific mechanism. *Molecular neurodegeneration*. Oct 19 2018;13(1):57.

4. Rudinskiy N, Grishchuk Y, Vaslin A, et al. Calpain hydrolysis of alpha- and beta2-adaptins decreases clathrin-dependent endocytosis and may promote neurodegeneration. *The Journal of biological chemistry*. May 1 2009;284(18):12447-58.

5. Wollmer MA. Cholesterol-related genes in Alzheimer's disease. *Biochimica et biophysica acta*. Aug 2010;1801(8):762-73.

6. Chen JJ, Li YM, Zou WY, Fu JL. Relationships between CETP genetic polymorphisms and Alzheimer's disease risk: a meta-analysis. *DNA and cell biology*. Nov 2014;33(11):807-15.

7. Wahrle SE, Jiang H, Parsadanian M, et al. ABCA1 is required for normal central nervous system ApoE levels and for lipidation of astrocyte-secreted apoE. *The Journal of biological chemistry*. Sep 24 2004;279(39):40987-93.

8. Pant S, Sharma M, Patel K, Caplan S, Carr CM, Grant BD. AMPH-1/Amphiphysin/Bin1 functions with RME-1/Ehd1 in endocytic recycling. *Nature cell biology*. Dec 2009;11(12):1399-410.

9. Liu CC, Liu CC, Kanekiyo T, Xu H, Bu G. Apolipoprotein E and Alzheimer disease: risk, mechanisms and therapy. *Nat Rev Neurol*. Feb 2013;9(2):106-18.